

CaloQVAE : Simulating high-energy particle-calorimeter interactions using hybrid quantum-classical generative models

Sehmimul Hoque^{a,1,2}, Hao Jia^{b,6}, Abhishek Abhishek^{4,6}, Mojde Fadaie¹, J. Quetzalcoatl Toledo-Marín⁴, Tiago Vale^{4,5}, Roger G. Melko^{c,1,2}, Maximilian Swiatlowski⁴, Wojciech T. Fedorko^{d,4}

¹Perimeter Institute for Theoretical Physics, Waterloo, Ontario N2L 2Y5, Canada

²Faculty of Mathematics, University of Waterloo, Ontario N2L 3G1, Canada

³Department of Physics and Astronomy, University of British Columbia, Vancouver, BC V6T 1Z1, Canada

⁴TRIUMF, Vancouver, BC V6T 2A3, Canada

⁵Department of Physics, Simon Fraser University, Vancouver, BC V5A 1S6, Canada

⁶Present Address: University of British Columbia

the date of receipt and acceptance should be inserted later

Abstract The Large Hadron Collider’s high luminosity era presents major computational challenges in the analysis of collision events. Large amounts of Monte Carlo (MC) simulation will be required to constrain the statistical uncertainties of the simulated datasets below these of the experimental data. Modelling of high-energy particles propagating through the calorimeter section of the detector is the most computationally intensive MC simulation task. We introduce a technique combining recent advancements in generative models and quantum annealing for fast and efficient simulation of high-energy particle-calorimeter interactions.

1 Introduction

The Large Hadron Collider (LHC) is the highest energy particle accelerator in the world, and currently collides protons at $\sqrt{s} = 13.6$ TeV with instantaneous luminosity of 2×10^{-34} cm²s⁻¹. Following the discovery of the Higgs Boson in 2012 [1, 2], significant advancements in measurements have been achieved, but in order to maximize the physics potential of the collider, an upgrade is underway to significantly increase the instantaneous luminosity to $5 - 7.5 \times 10^{-34}$ cm²s⁻¹. This “High-Luminosity LHC” (HL-LHC) dataset will enable significantly more precise measurements of the Higgs boson and other Standard Model particles, and will facilitate searches for new phenomena.

The significant increase in the rate of data-taking presents a computational challenge in the generation of sufficient high-quality simulated datasets, which are typically used to both calibrate the detectors and evaluate compatibility of the data with different physical hypotheses. These

simulated datasets are produced with first-principles particle simulation software in the GEANT4 framework [3], though less-accurate, parameterized models of the detectors, often called “fast simulation”, are also used [4]. The increased rate of data-taking and precision required to exploit the high-statistics HL-LHC dataset demands both that the computational time to produce simulated datasets decrease, and that the quality of the simulation remains as close as possible to that of the first-principles simulation [5].

A significant portion of the computational burden of the simulation lies in the interaction of particles with the calorimeter subsystems. Calorimeters are detectors that measure particle energies via the production of showers and the subsequent measurement of those showers as they traverse the active material of the detector. The ATLAS and CMS detectors both contain “Electromagnetic” calorimeters dedicated to the measurement of photons and electrons, and “Hadronic” calorimeters dedicated to measuring hadrons (typically π^\pm , protons, and neutrons). The accurate simulation of these complicated particle showers is critical to enable the highest quality measurements, but simulating each shower from first principles is very time consuming. This has motivated in recent years several approaches to reproduce these showers via machine-learning-based methods.

Recently, significant advancements have been made in various machine-learning domains related to generative models. In the development of variational autoencoders (VAEs) and their extensions, a series of breakthroughs have shaped the field [6, 7, 8, 9]. The development of the generative models provides inspiration to collider physics in the context of calorimeter simulation. In 2018, novel techniques based on generative adversarial networks (GANs) were developed to address the need for fast simulation of electromagnetic showers in calorimeters [10]. In 2021, the

^ae-mail: s4hoque@uwaterloo.ca

^be-mail: haojia@phas.ubc.ca

^ce-mail: rmelko@perimeterinstitute.ca

^de-mail: wfedorko@triumf.ca (corresponding author)

advancements have introduced innovative frameworks like CaloFlow based on normalizing flows, offering fast and accurate simulations with high fidelity and stability [11]. Most recently, IEA-GAN combines Self-Supervised Learning with Generative Adversarial Networks to efficiently simulate ultra-high-resolution particle detector responses with a relational reasoning module [12].

In traditional generative models, the computational costs and the time required for GPU processing in Markov Chain evaluations are significant concerns. Therefore, we aim to develop a quantum-assisted generative model for calorimeter data simulation, inspired by the potential of quantum computing to reduce these computational burdens. In 2015, a method utilising quantum annealing for training deep neural networks was proposed with a description on how to map Restricted Boltzmann Machines onto a D-Wave Two hardware [13]. Building on this idea, a subsequent work explored quantum annealers' ability to sample from Boltzmann distributions [14]. The development of the quantum variational autoencoder (QVAE) showcased the feasibility of utilising a quantum Boltzmann machine as a prior for latent generative process in a variational autoencoder [15, 16]. In 2021, a hybrid quantum-classical qGAN showed promise for accelerating HEP detector simulations using quantum generator circuits and classical discriminator neural networks [17]. In a very recent development, CaloDVAE introduced a discrete variational autoencoder with an RBM prior for fast calorimeter shower simulation, yielding promising results in generating realistic and diverse samples. The possibility of using quantum annealing processors as sampling devices for the RBM prior was also discussed [18].

In this paper, we extend the previous work from CaloDVAE to CaloQVAE by employing the D-Wave quantum hardware [19] to get samples from the latent space in a classically trained Variational Autoencoder (VAE), thereby bypassing the need for computationally intensive Markov Chain evaluations used in shower model simulations. To our knowledge, this approach marks the first instance of utilizing quantum computing to generative models for calorimeter shower simulations at a realistic scale.

2 Model Setup

Variational Autoencoders (VAEs) are a class of latent variable generative models, that maximize an evidence lower bound (ELBO) to the true log-likelihood [6]:

$$\log p_{\theta}(\mathbf{x}) \geq \mathbb{E}_{q_{\phi}(\mathbf{z}|\mathbf{x})}[\log p_{\theta}(\mathbf{x}|\mathbf{z})] - \text{KL}[q_{\phi}(\mathbf{z}|\mathbf{x})||p(\mathbf{z})] \quad (1)$$

Equation 1 is the ELBO for the original unconditional VAE framework. $\text{KL}[Q||P]$ is the Kullback-Liebler divergence between two probability distributions, Q and P while \mathbb{E}_p denotes an expectation value over the distribution p . The variables \mathbf{x} and \mathbf{z} represent data (in this case a vector of calorimeter cell energies) and latent variable respectively.

The approximating posterior, $q_{\phi}(\mathbf{z}|\mathbf{x})$ and the generative, $p_{\theta}(\mathbf{x}|\mathbf{z})$ distributions are often parameterized using neural networks with parameters ϕ and θ . In the original VAE framework [6], $p(\mathbf{z})$, the prior distribution of the VAE, is the standard Gaussian Distribution $\mathcal{N}(\mathbf{0}, \mathbf{I})$, while $q_{\phi}(\mathbf{z}|\mathbf{x})$ is parameterized by the distribution, $\mathcal{N}(\boldsymbol{\mu}_{\phi}(\mathbf{x}), \boldsymbol{\Sigma}_{\phi}^2(\mathbf{x}))$ with mean $\boldsymbol{\mu}_{\phi}(\mathbf{x})$ and covariance $\boldsymbol{\Sigma}_{\phi}^2(\mathbf{x})$.

CaloDVAE [7] is a hierarchical discrete VAE which extends the VAE framework by introducing discrete latent variables $\mathbf{z}_i \in \{0, 1\}$ in the latent space. Equation 1 is the loss for the unconditional VAE model. For conditional VAEs the encoder and decoder have an additional conditioning variable. In our case the encoder, $q_{\phi}(\mathbf{z}|\mathbf{x}, \mathbf{e})$, and decoder, $p_{\theta}(\mathbf{x}|\mathbf{z}, \mathbf{e})$, are conditioned on energy \mathbf{e} [18, 20] (unlike the encoders and decoders of Equation 1 of the unconditional VAE framework) and are modelled by fully connected neural networks. The approximate posterior of the VAE has a hierarchical structure $q_{\phi}(\mathbf{z}|\mathbf{x}, \mathbf{e}) = \prod_i q_{\phi_i}(\mathbf{z}_i|\mathbf{z}_{j<i}, \mathbf{x}, \mathbf{e})$ with N latent groups and the latent distribution of the VAE is modelled by an RBM where $\mathbf{z} = [\mathbf{z}_1, \dots, \mathbf{z}_N]$ are partitioned into 2 equal subsets to make the 2 sides of the RBM [18]. The RBM is modeled by probability distribution $p_{RBM} = e^{\mathbf{a}_l^T \mathbf{z}_l + \mathbf{a}_r^T \mathbf{z}_r + \mathbf{z}_l^T \mathbf{W} \mathbf{z}_r} / Z$ where Z is the partition function and $(\mathbf{a}_l, \mathbf{a}_r, \mathbf{W})$ are the RBM parameters which are trained along with the VAE parameters (θ, ϕ) .

At first VAE and RBM parameters are jointly trained using the standard VAE objective and a binary cross-entropy (BCE) loss to enhance the generative capability of the model. For the BCE loss, firstly binary labels are created to isolate pixel positions with non-zero energy values in the energy images. Subsequently, a BCE loss is computed between the binary label of the preprocessed input data and the binary label of the reconstructed data to incentivize the VAE to faithfully reproduce the distribution of non-zero energy pixels [18]. Furthermore, due to non-differentiability of discrete values we replace discrete values with continuous variables following the Gumbel trick to allow backpropagation during training [9]. Therefore the latent discrete variables \mathbf{z} are replaced with continuous proxy variables ζ with the Gumbel trick. Similarly we also apply Gumbel trick on reconstructed labels to mask the reconstructed energies. Finally in inference the continuous variables are replaced with the discrete variables [18].

We obtain a trained model with trained VAE and RBM parameters using the prescription above. The next step is to generate latent RBM samples, \mathbf{z} , and pass the samples through the trained VAE decoder to obtain the shower images. In CaloDVAE, block Gibbs sampling is used to generate the latent RBM samples. In CaloQVAE, we propose a novel calorimeter simulation framework based on the quantum variational autoencoder generative model to generate latent space samples, instead of using computationally expensive block Gibbs sampling.

3 CaloQVAE Training and Inference

In this work we demonstrate that we can generate latent space samples using the D-Wave 2000Q annealer. The first step to use the quantum processing unit (QPU) in the pipeline is to embed the RBM on the quantum hardware. However, the QPU architecture is not fully connected and instead follows a Chimera graph topology, making it impractical to natively embed a fully connected RBM in the QPU [13]. We therefore create a masking function to remove selected edges from an RBM to produce a Chimera RBM. We train the model classically analogously to the CaloDVAE training by replacing the RBM of CaloDVAE with a Chimera RBM.

In the inference phase we first convert the Chimera RBM Hamiltonian to an Ising model Hamiltonian \mathcal{H}_P using a linear transformation [21]. We embed the Chimera RBM on the QPU, and anneal according to the QPU Hamiltonian $\mathcal{H}(s) = A(s)\mathcal{H}_T + B(s)\mathcal{H}_P$, where $\mathcal{H}(s)$ is the total Hamiltonian of system at the re-scaled time s of annealing, \mathcal{H}_T is the transverse field Hamiltonian, $A(s)$ and $B(s)$ are monotonic functions [22]. We anneal $\mathcal{H}(s)$ for 20 μs following the standard D-Wave annealing schedule. During the anneal a freezing point s^* is typically observed on the device [23,24], after which $A(s^*) \ll B(s^*)$ and the change in dynamics becomes negligible. If the time taken to freeze is sufficiently short, the device output configurations x will approximately follow a Boltzmann Distribution at s^* , with $P(x) \propto \exp(-\beta_{eff}^* \mathcal{H}_P(x))$. This defines an effective inverse temperature β_{eff}^* [13,25] which is discovered to be instance-dependent and fluctuate at different programming cycles [26]. Therefore, a real-time β_{eff}^* estimation is needed [27]. In our work we estimate β_{eff}^* using an iterative procedure [16] where we first generate samples from the trained Chimera RBM classically using Block Gibbs Sampling. We then iteratively generate synthetic samples from the QPU while adjusting β_{eff}^* and then rescaling the QPU parameters (couplings and local fields) by β_{eff}^* until the quantum energy distribution converges to the classical energy distribution [16]. Figure 1 shows energy distributions for the QPU samples and classical samples.

4 Performance Evaluation

For training and performance evaluation we use the public CaloGAN dataset [28] simulated from GEANT4 [3]. The dataset provides 100,000 events for π^+ , γ and e^+ incident particles [10] and is split into 80%, 10%, and 10% subsets for training, validation, and testing, respectively. After conducting a hyperparameter scan [18], we obtain the best models for each particle type. Utilizing classical blocked Gibbs sampling and QPU sampling methods respectively, we generate new samples from the latent space and pass them through the decoder to obtain synthetic shower images. These images are then compared with GEANT4 test data

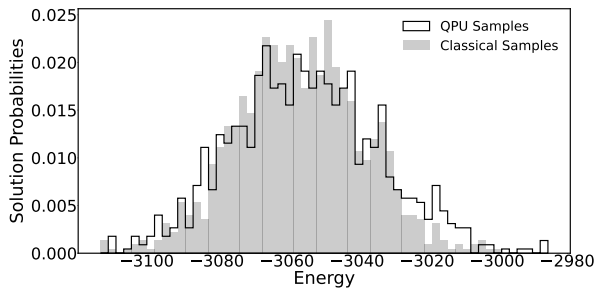


Fig. 1 Histogram showing the probability of obtaining sample s with Ising Energy computed by $E(s) = s^T J s + h^T s$ in dimensionless units for a trained CaloQVAE model. The energy distribution of QPU samples (solid line) are very close to the classical samples (shaded) after accounting for the β_{eff}^* factor.

to assess their performance. Classification can be used as a useful indicator of the performance of generative models. A good classifier should be able to understand and capture the important patterns in the data because it needs to learn discriminating features that distinguish different classes or categories accurately. We perform binary classification of e^+ vs π^+ and e^+ vs γ using a neural network with 6 fully connected layers with dropout, following the method of [10]. All synthetic data is generated from the QPU using separate models trained separately on e^+ , π^+ and γ samples. Our accuracy metrics (Table 1) are very close to the results obtained in [10]. The similar accuracy metrics illustrate that our CaloQVAE model is generating synthetic data that captures important patterns present in the true data, which indicates that the synthetic images generated from the QPU are successful at representing the underlying structure and characteristics of the true data. The fact that the classifier trained on synthetic e^+ vs π^+ data can perform well when tested on the GEANT4 data, and vice versa, suggests that the features learned by the CaloQVAE model are transferable. This means that the CaloQVAE model has successfully encoded the relevant information from the true data into its latent space representation, which allows the generated data to be informative and useful for training a classifier. An issue that requires attention is the unexpected high performance of the e^+ vs γ classifier, which is trained with synthetic data and tested on a separate set of synthetic data. Similar over-performance has also been observed in [10]. This raises the possibility that our CaloQVAE model may generate certain non-physical features, which allow the classifier to distinguish between the e^+ and γ samples. Further research is warranted to explore potential ways of addressing this challenge.

We qualitatively analyze one-dimensional histograms of the typical shower shape variables. As shown in Fig 2, there is a close alignment between the results from GEANT4 data

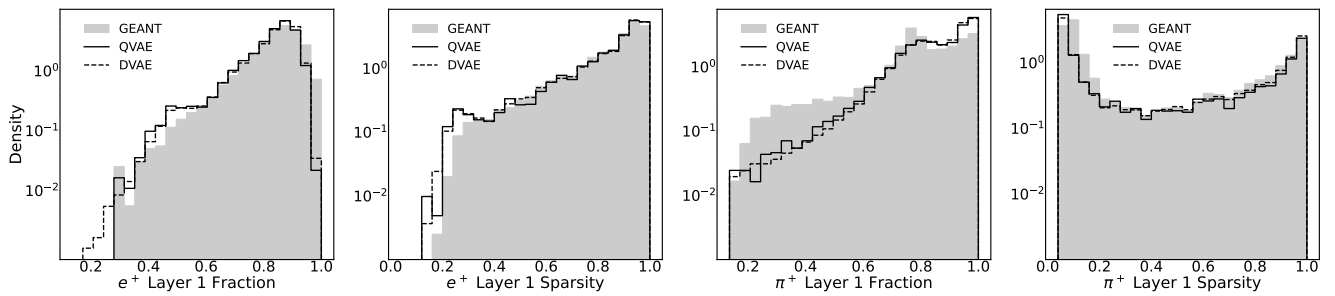


Fig. 2 Comparison of shower shape variables for π^+ and e^+ particles in a calorimeter. This figure shows the distributions of two key variables: (1) Fraction of energy: The energy deposited in the first layer compared to the sum of energy in all layers. (2) Sparsity: The ratio of the number of hits in the first layer to the total number of hits in all layers. Each variable is plotted for both particle types to illustrate the close alignment among the results from GEANT4, DVAE (classical) and QVAE (quantum) models.

Table 1 Binary classification accuracy for e^+ vs π^+ and e^+ vs γ where we train and test both on the Geant4 data and synthetic data produced from QPU samples

		e^+ vs π^+		e^+ vs γ	
		Test		Test	
Train	Geant4	99.8	99.9	66.8	74.1
	Synthetic	94.3	100.0	53.7	99.9

and generative models, which signifies that our generative model effectively captures the underlying patterns and distributions of the data. The consistent distribution patterns highlight the generative model’s fidelity in representing the essential features in the training dataset. Despite the observation of tail differences at the low fraction region for the positron in layer 1’s fraction histogram, the overall similarity between the performance of QVAE and DVAE models indicates our pipeline for Beta estimation and scaling is well behaved so that the quality of samples from the quantum device is on par with those from the Blocked Gibbs Method.

To assess the practical deployment performance of the model’s energy conditioning, we generate samples from the trained model requesting a specific range of incident energy and histogram the observed energy. We generate the samples by classical and quantum approaches and compare the results with a GEANT4 test dataset under the same range of incident energy. As shown in Fig 3, for the positron cluster, the conditioning response of DVAE or QVAE can form a flat plateau with good accuracy in reproducing the defined selection of the input energy range. The pion cluster has a broadened response that is due to the nature of the unconstrained charged pion shower in the electromagnetic calorimeter. The histograms of the generative models for both electron and pion clusters are able to mirror the characteristics observed in the true data. This compelling agreement underscores the VAE’s ability to capture and faithfully reproduce the intricate patterns inherent in the first-principles simulation,

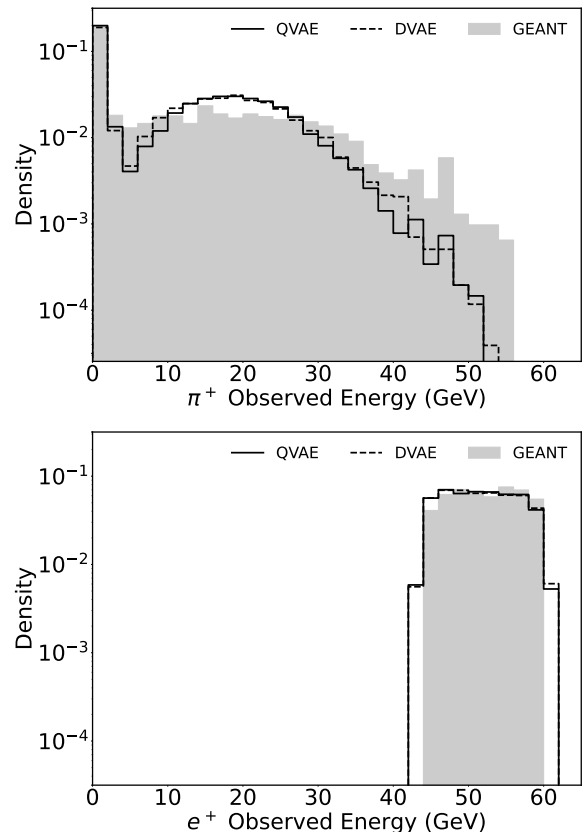


Fig. 3 Comparison of energy spectra between CaloDVAE (classical) and CaloQVAE (quantum) models against GEANT4 test data for incident particle energies ranging from 45 to 60 GeV. The data encompasses both positron and pion clusters.

thereby affirming its efficacy as a powerful tool for energy pattern generation.

The monitoring results of the DVAE sampling rate show efficient performance on our NVIDIA GeForce RTX 2080 Ti with 11264 MB memory. The processing time per sample for latent space sampling takes the most substantial portion (~ 0.5 ms), followed by data loading to the GPU (~ 10 ns), and passing through the decoder ($\sim 1 \mu\text{s}$). The DVAE

model exhibits similar sampling rate with the CaloGAN results [10] up to an order of magnitude. On the other hand, the quantum sampler achieves slightly faster sampling rate at 0.4 ms per sample, but impressively, the core QPU annealing rate is only 20 μ s per sample, hinting at the raw speed of quantum processing. The extra QPU access time is mainly used for tasks like readout and handling delays, suggesting that with optimized engineering, quantum sampling could vastly outpace classical methods in efficiency for generative modeling, making it well-suited for real-time and large-scale applications. We expect to apply the QVAE model to more complex objects, jets and events in the future, for which annealing time is expected to remain at the current level.

5 Conclusion

This work is the first demonstration of the application of a quantum annealing device to the computationally expensive simulation of particle showers at the Large Hadron Collider. We have shown that it is possible to utilize the Quantum Processing Unit (D-Wave Chimera 2000Q) to generate RBM samples which can be used to generate particle showers. The resulting generated simulation is able to largely match the properties of the training dataset, and match the performance of other generative models. The raw QPU annealing time per sample is measured to be 20 μ s, which is 20 times faster than generating samples via GPU. While further work remains in evaluating on more realistic simulation and a wider range of physics topologies, the initial results demonstrate CaloQVAE to be a promising application of quantum computing to open research questions in fundamental physics.

Acknowledgements The authors would like to thank Drs. Walter Vinci, Mohammad Amin, Geoffrey Fox, the members of the DeGeSim Collaboration as well as the members of the Perimeter Institute Quantum Intelligence Lab for many enlightening discussions. We thank Dr O. Di Matteo for early project conceptualization and material support for A. Abhishek during the final stages of the research. This work is supported by the Natural Sciences and Engineering Research Council of Canada (NSERC), National Research Council (NRC) and the Canadian Institute for Advanced Research (CIFAR) AI chair program. Research at Perimeter Institute is supported in part by the Government of Canada through the Department of Innovation, Science and Economic Development Canada and by the Province of Ontario through the Ministry of Economic Development, Job Creation and Trade. We gratefully acknowledge funding from the NRC via Agreement AQC-002, NSERC, including via grants SAPPJ-2020-00032, SAPPJ-2022-00020, and RGPIN-2022-04609 This research was enabled in part by computational support provided by the Shared Hierarchical Academic Research Computing Network (SHARCNET) and the Digital Research Alliance of Canada.

S.H. and H.J. contributed equally to this work and are listed in alphabetical order.

Data Availability Statement The analytical results and code are available online [29].

References

1. ATLAS Collaboration, Physics Letters B **716**(1), 1 (2012). DOI

- 10.1016/j.physletb.2012.08.020. URL <https://doi.org/10.1016%2Fj.physletb.2012.08.020>
2. CMS Collaboration, Physics Letters B **716**(1), 30 (2012). DOI 10.1016/j.physletb.2012.08.021. URL <https://doi.org/10.1016%2Fj.physletb.2012.08.021>
3. S. Agostinelli, et al., Nucl. Instrum. Meth. A **506**, 250 (2003). DOI 10.1016/S0168-9002(03)01368-8
4. ATLAS Collaboration, Comput. Softw. Big Sci. **6**(1), 7 (2022). DOI 10.1007/s41781-021-00079-7
5. ATLAS Collaboration, ATLAS HL-LHC Computing Conceptual Design Report. Tech. rep., CERN, Geneva (2020). URL <https://cds.cern.ch/record/2729668>
6. D.P. Kingma, M. Welling. Auto-Encoding Variational Bayes (2022). arXiv:1312.6114
7. J.T. Rolfe. Discrete Variational Autoencoders (2017). arXiv:1609.02200
8. A. Vahdat, et al., in *International Conference on Machine Learning* (PMLR, 2018), pp. 5035–5044
9. A.H. Khoshaman, M.H. Amin, arXiv:1805.07349 (2018)
10. M. Paganini, L. de Oliveira, B. Nachman, Phys. Rev. D **97**(1), 014021 (2018). DOI 10.1103/PhysRevD.97.014021
11. C. Krause, D. Shih, Phys. Rev. D **107**, 113003 (2023). DOI 10.1103/PhysRevD.107.113003. URL <https://link.aps.org/doi/10.1103/PhysRevD.107.113003>
12. H. Hashemi, N. Hartmann, S. Sharifzadeh, J. Kahn, T. Kuhr. Ultra-high-resolution detector simulation with intra-event aware gan and self-supervised relational reasoning (2023). arXiv:2303.08046
13. S.H. Adachi, M.P. Henderson, arXiv e-prints arXiv:1510.06356 (2015)
14. M. Benedetti, J. Realpe-Gómez, R. Biswas, A. Perdomo-Ortiz, Phys. Rev. A **94**, 022308 (2016). DOI 10.1103/PhysRevA.94.022308. URL <https://link.aps.org/doi/10.1103/PhysRevA.94.022308>
15. A. Khoshaman, W. Vinci, B. Denis, E. Andriyash, H. Sadeghi, M.H. Amin, Quantum Science and Technology **4**(1), 014001 (2018). DOI 10.1088/2058-9565/aada1f. URL <https://doi.org/10.1088%2F2058-9565%2Faada1f>
16. W. Vinci, L. Buffoni, H. Sadeghi, A. Khoshaman, E. Andriyash, M.H. Amin, Machine Learning: Science and Technology **1**(4), 045028 (2020). DOI 10.1088/2632-2153/aba220. URL <https://dx.doi.org/10.1088/2632-2153/aba220>
17. F. Rehm, S. Vallecorsa, K. Borras, D. Krücker, in *9th International Conference on Distributed Computing and Grid Technologies in Science and Education* (2021), pp. 363–368
18. A. Abhishek, E. Drechsler, W. Fedorko, B. Stelzer. CaloDVAE : Discrete Variational Autoencoders for Fast Calorimeter Shower Simulation (2022). arXiv: 2210.07430
19. D-Wave Systems. Getting Started with D-Wave Solvers. https://docs.dwavesys.com/docs/latest/doc_getting_started.html
20. ATLAS Collaboration, Deep generative models for fast shower simulation in ATLAS. Tech. rep., CERN, Geneva (2018). URL <https://cds.cern.ch/record/2630433>
21. V. Dixit, R. Selvarajan, T. Aldwairi, Y. Koshka, M.A. Novotny, T.S. Humble, M.A. Alam, S. Kais, IEEE Transactions on Emerging Topics in Computational Intelligence **6**(3) (2022). DOI 10.1109/tetci.2021.3074916
22. M.H. Amin, E. Andriyash, J. Rolfe, B. Kulchytskyy, R. Melko, Physical Review X **8**(2), 021050 (2018)
23. M.H. Amin, Phys. Rev. A **92**, 052323 (2015). DOI 10.1103/PhysRevA.92.052323. URL <https://link.aps.org/doi/10.1103/PhysRevA.92.052323>
24. J. Marshall, E.G. Rieffel, I. Hen, Phys. Rev. Appl. **8**, 064025 (2017). DOI 10.1103/PhysRevApplied.8.064025. URL <https://link.aps.org/doi/10.1103/PhysRevApplied.8.064025>

25. A. Perdomo-Ortiz, B. O’Gorman, J. Fluegemann, R. Biswas, V.N. Smelyanskiy, Scientific Reports **6** (2015)
26. J. Marshall, E.G. Rieffel, I. Hen, Phys. Rev. Appl. **8**, 064025 (2017). DOI 10.1103/PhysRevApplied.8.064025. URL <https://link.aps.org/doi/10.1103/PhysRevApplied.8.064025>
27. G. Xu, W.S. Oates, Scientific Reports **11**(1) (2021). DOI 10.1038/s41598-021-82197-1. URL <https://www.osti.gov/biblio/1816563>
28. B. Nachman, L. de Oliveira, M. Paganini. Electromagnetic calorimeter shower images (2017). DOI 10.17632/pvn3xc3wy5.1
29. QaloSim. GitHub Repository (2023). URL <https://github.com/QaloSim/CaloQVAE/tree/chimera-dwave-sampling>